Decay of ^{145}Cs to levels of ^{145}Ba

J. D. Robertson, S. H. Faller, and W. B. Walters
Department of Chemistry, University of Maryland, College Park, Maryland 20742

R. L. Gill, H. Mach, and A. Piotrowski*
Physics Department, Brookhaven National Laboratory, Upton, New York 11973

E. F. Zganjar
Department of Physics, Louisiana State University, Baton Rouge, Louisiana 70805

H. Dejbakhsh† and R. F. Petry
Department of Physics, University of Oklahoma, Norman, Oklahoma 73019
(Received 28 April 1986)

An investigation of the β^- decay of 0.59 s ^{145}Cs into levels of ^{145}Ba was undertaken to search for evidence of intrinsic reflection asymmetry in light rare-earth nuclei. E_γ, I_γ, γ-γ coincidence, angular correlation coefficients, and internal conversion coefficients were measured. The level scheme for ^{145}Ba up to 1.3 MeV has been constructed. The proposed spin and parity assignments are based upon the measured transition multipolarities and the γ-γ angular correlation coefficients. The levels at 112, 175, 277, and 416 keV may be members of a decoupled $K=\frac{1}{2}^-$ band with a decoupling parameter of -2 and a rotational parameter of 20 keV. The octupole deformed rotational structure which is observed in the light odd-A actinides is not readily identified in ^{145}Ba.

I. INTRODUCTION

In 1950 Rainwater proposed that the discrepancy between the measured and calculated values of the quadrupole moments of some odd-A nuclei could be resolved by allowing those nuclei to take on a spheroidal shape.[1] It is now well known that the properties of many nuclei can be described with a deformed quadrupole basis. Over the past few years, much attention has been focused on the question of whether or not some nuclei, in addition to breaking rotational symmetry in the intrinsic frame, also break reflection symmetry. The nuclei in question are found in the Ra and Th region with mass ranging from 220 to 228. A review of the extensive literature on this region can be found in Refs. 2–8.

In a recent paper, Leander *et al.* introduced the idea that nuclei with $N=88$–90 in the immediate vicinity of ^{145}Ba might exhibit the same type of octupole deformed character that is observed in the $Z=89$–90 light actinide region.[9] Three reasons are given as to why this might be a new region where reflection symmetry is also broken in the intrinsic frame. First of all, the systematics of the 1^- and 3^- levels in the neutron rich Ba isotopes suggest a minimum in the splitting of the $K^\pi=0^+$ and 0^- bands near ^{146}Ba. The 1^- level in ^{146}Ba at 738 keV, in units of the first 2^+ level, is as low as the 1^- levels in the Ra and Th isotopes. It was the discovery of these low-lying negative parity states in the even-even Ra isotopes that first led to the suggestion that nuclei in the Ra and Th region were octupole deformed.[10] Secondly, the deformed shell model calculations of Nazarewicz *et al.* indicate that $Z=56$, as well as Z or $N=88$–90, is an optimal particle number for octupole deformation.[5] The Strutinsky-type calculations predict an octupole deformed shape for ^{146}Ba and a shape potential for ^{144}Ba that is very soft towards octupole deformation. Finally, the large difference observed between the experimental and theoretical masses calculated by Möller and Nix in the Ra and Th regions are also found near ^{145}Ba.[2] This difference is greatest for ^{145}Ba and, as in the light actinide region, can be accounted for by the extra 1 MeV of binding energy obtained by including octupole correlations in the mass calculations.

The ground state (g.s.) spin of ^{145}Ba has been determined to be $\frac{5}{2}$ by collinear fast-beam laser spectroscopy at ISOLDE.[11] A g.s. magnetic moment or $-0.272\mu_N$ and a spectroscopic quadrupole moment (Q_S) of 1.15 b is reported in the same work. From the measured g.s. spin and Q_S value, Leander *et al.* calculate that ^{145}Ba may be octupole deformed with an equilibrium value of $\beta_3\cong 0.08$ (with $\beta_2=0.172$ and $\beta_4=0.069$).[9] However, the measured magnetic moment is consistent with both $\beta_3=0$ and $\beta_3\neq 0$ in the calculations.

Another indication of octupole deformation in the neutron rich Ba isotopes would be the presence of a pair (or more) of strongly perturbed opposite-parity rotational bands in ^{145}Ba. If unperturbed, the bands would have a small energy splitting and be connected by collective $E1$ transitions. In addition, the decoupling parameters for any $K=\frac{1}{2}^\pm$ bands should be equal in magnitude but opposite in sign.[12] This type of collective structure is observed in both ^{225}Ra and ^{227}Ac (Fig. 1).[13,14]

In a previous study of ^{145}Ba, Rapaport *et al.* found one $E1$ transition but did not identify any rotational bands.[15] In their study, however, only 31 gamma rays were assigned to the β^- decay of ^{145}Cs and the structure of ^{145}Ba was only determined up to 780 keV from energy

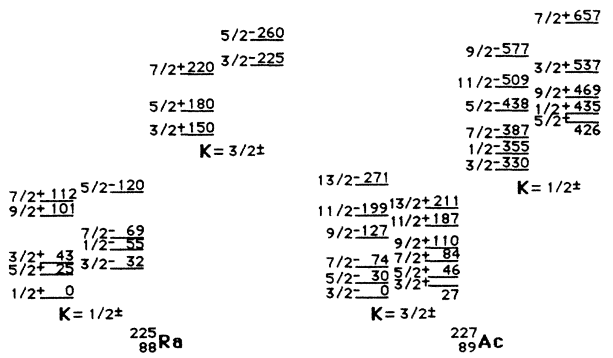

FIG. 1. The parity doublets observed in the light actinides ^{225}Ra and ^{227}Ac (Refs. 13 and 14).

sum relationships. A later investigation of ^{145}Cs decay by Dejbakhsh defined the structure of ^{145}Ba up to 2.8 MeV from γ-γ coincidence measurements.[16] Unfortunately, no new spins or parities could be assigned in the latter study. Thus, to determine whether or not ^{145}Ba does contain parity doublets similar to those observed in the light actinides, we undertook a study of the β^- decay of ^{145}Cs at the one-line mass separator facility TRISTAN. Our study of ^{145}Cs decay principally involved γ-γ coincidence and four-detector angular correlation measurements. In addition, we also measured internal conversion coefficients for several of the most intense transitions in ^{145}Cs decay.

II. EXPERIMENTAL PROCEDURE

The study of the β^- decay of 0.59 s ^{145}Cs was conducted at the TRISTAN mass separator on-line to the High Flux Beam Reactor at Brookhaven National Laboratory.[17] The radioactive samples were produced by fissioning a uranium target integrated in a positive surface ionization source with a Ta ionizer.[18] The lower work function of Ta (compared to Re) ensured no independent production of Ba from the ion source at low-power operation ($T \simeq 1200$ °C).

In both the γ-ray and conversion electron (c.e.) measurements, the $A=145$ radioactive beam was deposited on an aluminized Mylar tape in a moving tape collector. The activity was measured at both the deposit point (parent port) and 60 cm "downstream" at a secondary station (daughter port) in the γ-ray experiments. In the c.e. measurements, the beam was deposited and counted at the parent port of a second collection system. For all of the studies, the beam deposit and tape cycle times were chosen so as to optimize the activity of the $A=145$ isobar of interest over the activity of the other chain members.

Two Ge(Li) and two HpGe detectors were used to collect the gamma singles and γ-γ coincidence data. The two coaxial Ge detectors were a 90 cm^3 Ge(Li) with a full width at half maximum (FWHM) of 2.2 keV at 1.33 MeV and a 79 cm^3 Ge(Li) with a FWHM of 2.4 keV at 1.33 MeV. The two coaxial hyperpure detectors were a 76 cm^3 HpGe with a FWHM of 2.2 keV at 1.33 MeV and a 79 cm^3 HpGe with a FWHM of 1.9 keV at 1.33 MeV. In addition, a 2 cm^3 planar detector with a FWHM of 0.55 keV at 122 keV was used to measure low-energy gammas. The SiLi detector used in the c.e. measurements has a resolution of 1.8 keV FWHM for the 662 keV K-shell conversion electron line in ^{137}Cs.

Singles spectra of ^{145}Cs decay were taken at the parent port with the best HpGe detector and the planar detector. In order to correct for the daughter activity observed in the ^{145}Cs singles spectra, singles spectra of each daughter in the $A=145$ chain (excluding Pr) were taken at the daughter port. To minimize the contribution of the parent activity to the total activity in the daughter singles, the radioactive source was moved half-way to the daughter port and allowed to decay before moving it on to the daughter port.

For the coincidence and angular correlation measurements, the four γ-ray detectors were placed around the parent port 7.5 cm from the radioactive source. The angles measured by the four detectors (six detector pairs) were one point at 0°, one point at 35°, two points at 55°, and two points at 90°. The two $0^+(E2)2^+(E2)0^+$ transitions in ^{142}Ba were used to test the four detector system. The $A=142$ activity was adjusted to be approximately equal to that of the $A=145$ samples. A total of 10^8 three parameter $\gamma\gamma t$ coincidence events were collected in the experiment.

III. EXPERIMENTAL RESULTS

A. Gamma-ray energies, relative intensities, and absolute intensities

The γ rays assigned to ^{145}Cs decay are listed in Table I. The assignments were based upon the appearance of the γ ray in (1) the ^{145}Cs singles spectra and (2) the coincidence spectra gated on the strongest transitions whose half-lives have been previously determined.[19] The contribution of the daughter gammas to the ^{145}Cs singles was identified and removed by comparing the intensities of the γ rays in each of the daughter singles with the Cs singles spectra. For the majority of the γ rays given in Table I, the energy and intensity values were determined from the singles data. In several cases, however, it was impossible to ascertain this information from the singles spectra because the intensity of the γ ray was too low or the γ ray was a member of a complex multiplet. In these instances, the energy and/or intensity values were determined from the coincidence spectra. The intensities of the 156-, 172-, and 199-keV γ rays were also taken from the coincidence data as these transitions overlap with strong lines in ^{144}Ba. The ^{144}Ba interference comes from the $(13.8\pm0.8)\%$ delayed neutron branch in ^{145}Cs decay.[20]

The absolute intensity values of the most intense gamma in ^{145}Cs, ^{145}Ba, and ^{145}La decay were determined by counting a saturated $A=145$ radioactive sample. The values listed in Table II were calculated by comparing the intensity of each γ ray to the 723-keV line from ^{145}Ce decay. The absolute intensity of the 723-keV gamma was taken as 0.59 ± 0.07 from the work of Pfeiffer *et al.*[21] This method of determining the absolute intensities assumes that all of the $A=145$ daughter activity comes from cesium decay, i.e., there is no independent production of Ba,

TABLE I. Gamma rays assigned to the decay of ^{145}Cs.

Energy (keV)[a]	Intensity[b]	σ Int.	Placement From	Placement To
38.24[c,d]	1.8	0.4	454.7	416.6
84.74	7.7	0.2		
86.26	5.8	0.1	198.9	112.5
87.34	2.28	0.04		
105.94[d]	0.79	0.09	672.4	566.7
112.46	54.1	0.7	112.5	0.0
121.01	0.4	0.2	319.8	198.9
156.34[c]	2.4	0.3	611.1	454.7
164.64[c]	7.5	0.6	277.1	112.5
171.97[e,f]	4.3	0.3	627.3	454.7
175.36	100.0		175.4	0.0
194.56	3.4	0.4	611.1	416.6
198.93[e]	55	9	198.9	0.0
207.12[c]	16.2	0.4	319.8	112.5
214.52	1.2	0.2	491.9	277.1
217.72	< 1		785.5	566.7
227.36	3.4	0.3	547.1	319.8
231.92[c]	1.8	0.2	724.3	491.9
238.41[c]	7.9	0.8	785.5	547.1
240.97	28.9	0.3	416.6	175.4
246.92	2.46	0.06	566.7	319.8
255.94	2.5	0.1	454.7	198.9
260.29[e]	0.9	0.2		
277.12	2.14	0.08	277.1	0.0
279.46	4.0	0.5	454.7	175.4
289.2	1.0	0.1	836.3	547.1
293.2	2.2	0.1	491.9	198.9
304.5	2.4	0.2	416.6	112.5
307.95	1.98	0.09	724.3	416.6
317.63	3.0	0.2	753.4	435.7
319.84	7.6	0.2	319.8	0.0
323.34	5.2	0.3	435.7	112.5
328.85[c]	1.9	0.2		
341.74[e]	0.6	0.1	454.7	112.5
343.44	4.2	0.2	663.3	319.8
348.21[e]	1.1	0.2	547.1	198.9
360.34[d,e]	1.0	0.2	796.0	435.7
367.71	5.3	0.2	566.7	198.9
369.18	0.87	0.09	785.5	416.6
378.93[c]	8.6	0.3	796.0	416.6
383.8	0.85	0.08	1137.9	753.4
391.15	1.1	0.3	566.7	175.4
395.14	5.6	0.6	672.4	277.1
416.52	5.1	0.8	416.6	0.0
419.74[d,e]	1.0	0.2	836.3	416.6
429.07[d,e]	1.3	0.4	627.3	198.9
430.27[f]	5.8	0.2	1155.3	724.3
434.71[e]	5.7	0.4	547.1	112.5
435.72[e]	10.2	0.9	611.1	175.4
435.63[c]	29.0	0.4	435.7	0.0
439.6[e]	4.5	1.1	1050.5	611.1
444.22[f]	0.60	0.06	1116.6	672.39
452.03[f]	8.8	0.5	627.3	175.4
454.28[e]	8.0	0.5	566.7	112.5
454.77	10.6	0.6	454.7	0.0
455.23[d,e]	1.4	0.4	1240.7	785.5
464.82[e]	1.0	0.2	663.3	198.9
473.76	1.0	0.2	1137.9	663.3
476.26	1.7	0.2	796.0	319.8
481.34	1.1	0.1	1353.5	872.3
487.18	6.9	0.2	663.3	175.4
492.08[e,f]	14.1	0.5	491.9	0.0
500.35	3.1	0.3	819.8	319.8
503.17	1.3	0.2	1050.5	547.1
517.24	1.0	0.1	1353.5	836.3
525.83	3.7	0.2	724.3	198.9
528.38[d,e]	8.7	1.1	1155.3	627.3
547.06	23.6	0.4	547.1	0.0
548.99	5.8	0.9	724.3	175.4
552.92[e,f]	1.6	0.4	872.3	319.8
554.73[c]	5.2	0.2	753.4	198.9
559.86	4.5	0.1	672.4	112.5
566.7	3.7	0.2	566.7	0.0
571.06	7.8	0.3	1137.9	566.7
574.05	0.7	0.2	851.5	277.1
578.13	7.6	2.4	753.4	175.4
586.61	1.8	0.3	785.5	198.9
595.46[e]	~1		872.3	277.1
597.48[e]	1.4	0.3	796.0	198.9
611.16	5.5	0.3	611.1	0.0
620.61	1.4	0.4	819.8	198.9
620.61	2.6	0.4	796.0	175.4
637.46	7.8	0.3	836.3	198.9
645.28	2.5	0.5	819.8	175.4
652.63	1.3	0.3	851.5	198.9
660.89	1.9	0.1	836.3	175.4
663.49[d]	2.0	0.2	663.3	0.0
683.44[c]	6.3	0.4	1137.9	454.7
688.48[c,d]	1.2	0.1	1299.6	611.1
693.09[d]	1.6	0.2	1240.7	547.1
700.62[c]	3.9	0.3	1155.3	454.7
706.63	2.1	0.2	819.8	112.5
721.13	5.1	0.3	1137.9	416.6
724.26[e]	8.1	3.1	724.3	0.0
739.1	4.6	0.2	1155.3	416.6
753.26	11.2	0.3	753.4	0.0
759.51	2.4	0.2	872.3	112.5
785.33	0.37	0.06	785.5	0.0
795.9	1.3	0.1	796.0	0.0
806.58	3.7	0.3	1353.5	547.1
819.68[d]	1.8	0.2	819.8	0.0
851.68[d]	1.2	0.2	851.5	0.0
872.13	1.7	0.3	872.3	0.0
875.03	1.2	0.2	1050.5	175.4
898.92[d,e]	1.2	0.4	1353.5	454.7
920.25[d]	0.9	0.1	1240.7	319.8
944.68[d]	1.1	0.3		
1034.02	2.7	0.2	1353.5	319.8
1066.38	3.2	0.2	1240.7	175.4
1101.12[d,e]	0.9	0.2	1299.6	198.9
1177.70[d,e]	1.8	0.6	1353.5	175.4
1240.30	1.08	0.02	1240.7	0.0
1414.45[d]	1.5	0.3		
1715.59[d]	2.8	0.4		
1976.94	9.0	0.5		
2024.33[d]	3.7	0.6		
2175.59	3.0	0.4		

TABLE I. (*Continued*).

[a]When two decimal places are reported, the uncertainty is ±0.02 keV for $E_\gamma > 100$ keV and ±0.06 keV for $E_\gamma < 100$ keV. When one decimal place is reported, the uncertainty is ±0.1 keV.
[b]For absolute intensity/100 decays multiply the intensity values by 0.20±0.02.
[c]I_γ corrected for daughter decay.
[d]Seen for the first time.
[e]I_γ taken from coincidence gates.
[f]Placed for the first time.

La, or Ce from the ion source. For Ba this assumption is supported, first of all, by gamma multiscaling data. At our operating conditions, the activity of ^{145}Ba as a function of time can be completely accounted for by growth from ^{145}Cs decay alone. Secondly, the Langmuir equation predicts that the ionization ratio of Cs^+/Ba^+ from a Ta surface at 1200°C should be 8000 to 1. For La and Ce, we know that neither are produced independently as studies at higher masses have shown that the source does not yield either element at our operating conditions. The absolute intensities of the 96- and 355-keV gammas given in Table II concur with the literature values.[21] In addition, the intensity of the 175-keV transition (γ+c.e.) agrees with the value of 24.4 reported by Rapaport *et al.*[15]

B. γ-γ coincidence and angular correlation measurements

A total of 131 summed coincidence spectra were generated by scanning the event-by-event data. For each energy gate, three coincidence spectra were produced for the best HpGe detector by setting the gate in each of the remaining three detectors. The resulting three spectra were then added together to enhance the coincidence intensities for each gate. As an example of summed coincidence spectra, a portion of the 112- and 175-keV gates are shown in Fig. 2.

The results of the angular correlation study are given in Table III. To account for the finite size of the detectors, solid angle correction factors (Q_2 and Q_4) were calculated for each detector pair using the method described by Camp and Van Lehn.[22] For each transition in Table II, an average $\overline{Q}_2$ and $\overline{Q}_4$ value were calculated and used to determine A_{22} and A_{44} ($A_{22}=A_{2\,\mathrm{expt}}/\overline{Q}_2$). The $\overline{Q}_2$ and $\overline{Q}_4$ values are of the order of 90% and 75%, respectively. For a given cascade, the standard deviation of $\overline{Q}_2$ and $\overline{Q}_4$ for the six detector pairs is 0.2% and 0.8%. Because the A_{22}/A_{44} values found for the two $0^+(E2)2^+(E2)0^+$ transitions in ^{142}Ba agree with the theoretical values (Table III), no other normalization factor was applied to the data.

TABLE II. Absolute intensity of the most intense gamma in the $A=145$ isobars.

Nuclide	E_γ (keV)	Abs. I_γ/decay[a]	Pfeiffer *et al.*	% Diff.
^{145}La	355.8	0.038±0.007	0.042±0.007	9
^{145}Ba	96.9	0.171±0.021	0.202±0.015	15
^{145}Cs	175.4	0.198±0.024		

[a]Values calculated assuming the absolute I_γ/decay of the 723-keV line from ^{145}Ce decay to be 0.59±0.07 (Ref. 21).

C. Internal conversion electron measurements

The conversion electron spectrum is shown in Fig. 3; no peaks were observed above channel 1760. The area of the 112-keV γ-ray peak in the SiLi detector, along with a γ-ray calibration curve for the SiLi detector, was used to determine the γ-ray intensities needed to calculate the internal conversion coefficients. The measured internal conversion coefficients, theoretical coefficients, and deduced multipolarities are summarized in Table IV. Because the 207-keV K electron peak overlaps with the strong 175-keV L electron peak, α_k for the 207-keV transition was calculated by assuming the 175-keV transition

TABLE III. Experimental angular correlation coefficients.

Cascade	A_{22}	A_{44}	X^2
	^{145}Ba		
86-112	0.51±0.04	−0.08±0.06	6.0
164-112	0.46±0.08	−0.07±0.10	8.2
207-112	−0.24±0.06	0.04±0.06	2.0
454-112	0.43±0.11	0.04±0.11	0.2
241-175	−0.02±0.04	0.06±0.03	26
279-175	−0.02±0.05	0.04±0.06	4.2
435-175	0.01±0.04	0.05±0.04	10
452-175	0.08±0.05	0.09±0.05	0.3
548-175	−0.01±0.06	0.12±0.04	3.3
578-175	−0.06±0.07	0.13±0.08	4.1
255-199	−0.32±0.08	0.03±0.08	7.1
367-199	0.13±0.05	0.21±0.05	1.4
554-199	−0.03±0.07	0.23±0.09	2.2
637-199	−0.39±0.08	0.47±0.13	1.8
194-241	−0.14±0.04	0.16±0.06	0.1
308-241	−0.22±0.08	0.38±0.10	0.7
721-241	−0.20±0.09	0.44±0.12	2.4
739-241	−0.05±0.06	0.26±0.08	1.5
317-435	−0.20±0.07	0.02±0.05	2.5
	^{142}Ba (0-2-0 cascades)		
1175-359	0.21±0.10	1.36±0.17	12
1280-359	0.15±0.09	1.17±0.06	18
Theor. 0-2-0	0.3571	1.143	

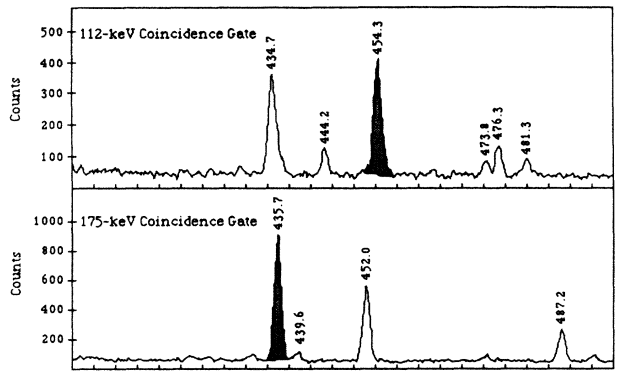

FIG. 2. Portions of the 112- and 175-keV γ-γ coincidence gates.

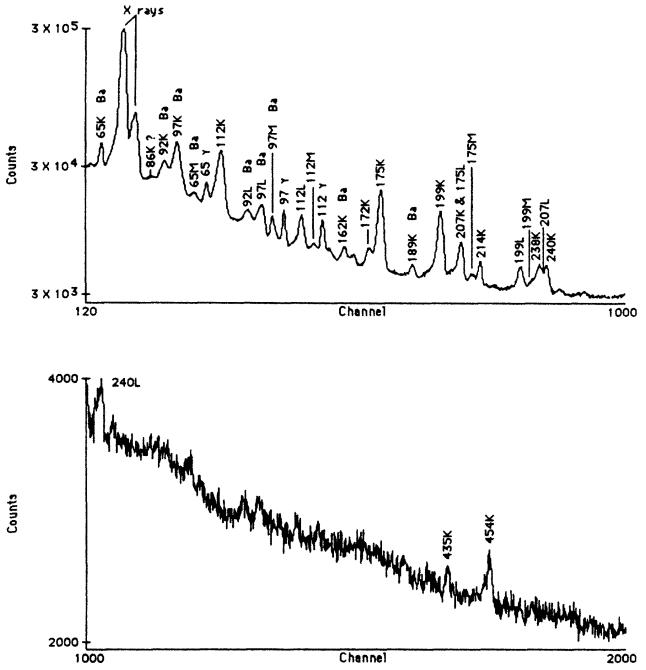

FIG. 3. The ^{145}Cs conversion electron spectrum. No peaks were observed above channel 2000.

to be pure $E2$ (see below). Likewise, the areas of the 199-keV K and 199-keV L electron peaks were corrected for the 199-keV $E2$ transition from the beta delayed neutron emission of ^{145}Cs to ^{145}Ba. The K-shell conversion coefficient reported in Table IV for the 454-keV transition is for the 454-keV gamma that feeds the ground state. The reported value was calculated by assuming the 566- to 112-keV and 1240- to 785-keV transitions to be $M1/E2$ in character. Because α_k for a 454-keV transition ranges only from 0.010 for a pure $E2$ to 0.014 for a pure $M1$, the median value of 0.012 was used for α_k in this calculation.

The K-shell conversion coefficient of 0.05 ± 0.02 for the 207-keV transition indicates that the 207-keV transition is an $E1$ transition. The large uncertainty in α_k is a result of the peak overlap mentioned above. Calculations show that the 547-keV K electron peak should have been observed if the 547-keV transition was $M1$ or $E2$. Because no peak was observed above the 454-keV K electron peak, we conclude that the 547-keV transition is $E1$. The conversion electron data also indicates that the transition from the 435-keV level to the g.s. is $E1$. The 435-keV transition that feeds the 175-keV level is known to be $E2$ from the angular correlation results (see below). In addition, the $E1$ character of the 547-keV gamma implies that the 547- to 112-keV transitions is $E1$. Correcting the 435-keV K electron peak for these two transitions yields an α_k of 0.0011 ± 0.0012 for the 435-keV to g.s. transition, consistent with an $E1$ assignment. Although the un-

TABLE IV. Experimental internal conversion coefficients ($\times10^2$).

Transition	Experimental conv. coef.	Rapaport[a]	Theoretical $M1$	Theoretical $E2$	Theoretical $E1$	Deduced multipolarity
86 K		0.571*[d]	7.6	1.8	7.3	$M1/E2$
112 K	91.9 ±12	78.8±24	58	84	14	$M1/E2$
L	12.8 ±1.2	13.8±4.1	8.4	34	1.9	
175 K	16.9 ±1.6	17.0±5.1	17	20	4.2	$E2$
M	0.74±0.08		0.5	1.1	0.1	
198 K	10.7 ±2.0	13.0±3.9	12	14	3.0	$M1/E2$
L	1.4 ±0.4	2.0±0.6	2.0	3.2	0.4	
207 K	5.3 ±2.0		11	12	2.7	$E1$
238 K	12.6 ±3.0	11.1±3.3	7.9	7.7	1.8	$M1/E2$
241 K	8.8 ±1.2	9.5±2.8	7.6	7.4	1.8	$E2$
L	0.8 ±0.1		1.1	1.7	0.2	
435 K[b]	0.11±0.12		1.5	1.1	0.4	$E1$
434 K[b]	0.11±0.12		1.5	1.0	0.3	$M1/E2$

[a]Reference 15.
[b]Conversion coefficient for the 435 to g.s. 435 keV transition.
[c]Conversion coefficient for the 454 to g.s. 454 keV transition.
[d]K/L ratio.

certainty in α_k is large, the 435-keV transition that feeds the g.s. must be $E1$, as calculations show that the area of the 435-keV K electron peak would have to be 3 times the observed value if a transition of this intensity (29.0) were $M1$ or $E2$ in character.

In contrast to the earlier work by Rapaport *et al.*,[15] we did not observe the 86-keV K electron peak (Fig. 3). Calculations predict that the area of the 86-keV K peak should be approximately 10% of the area of the 112-keV peak if the 86-keV transition is an $M1/E2$ transition. The absence of the peak suggests that either the relative intensity of the 86-keV γ ray is incorrect or that the multipolarity of the transition is $E1$ rather than $M1/E2$. Because the (86 keV)/(199 keV) intensity ratio in the 255-, 367-, and 554-keV coincidence gates is constant, it is unlikely that the relative intensity of the 86-keV γ ray is incorrect. Likewise, it is doubtful that the 86-keV transition is $E1$, as the c.e. data clearly indicate that both the 199- and 112-keV transitions are $M1/E2$ transitions (Table IV). This discrepancy can be resolved by assuming that the 86-keV K peak is buried in the shoulder of the 31-keV x-ray and 92-keV K electron peaks; i.e., the background between these two peaks is not flat but is actually filled with the 86-keV K electron peak. It should be noted, however, that our data can not rule out the possibility that the 86-keV transition is $E1$.

D. Beta branching

The beta feeding to each level was calculated as the difference between the transition intensity (γ+c.e.) feeding into and out of the level. For the majority of the transitions, the intensity was set equal to the gamma intensity as the electron contribution is negligible. The experimental conversion coefficients were used to calculate the transition intensity for the 112-, 199-, 207-, and 238-keV gamma rays and the theoretical coefficients were used for the 175- and 241-keV $E2$ transitions. In addition, the conversion coefficient reported by Rapaport *et al.* was used to calculate the intensity of the 86-keV transition.[15] The intensity value for the 38-keV transition is the median of the upper and lower limits for the transition. The limits were calculated by assuming α_{total} ranged from 2.4 (pure $M1$) to 5.1 (4% $E2$); at the maximum value of 5.1 there is zero beta feeding to the 416-keV level. The g.s. beta feeding of (2.9±3.0)% is in good agreement with the previously determined value of (3.2±2.0)%.[15]

E. Construction of the decay scheme

The level diagram proposed for ^{145}Ba is shown in Figs. 4–6. The logf_0t values were calculated from the compilation of Gove and Martin[23] with Q_β=7.95±0.08 MeV.[24] As can be seen in Figs. 4–6, all but two of the levels are

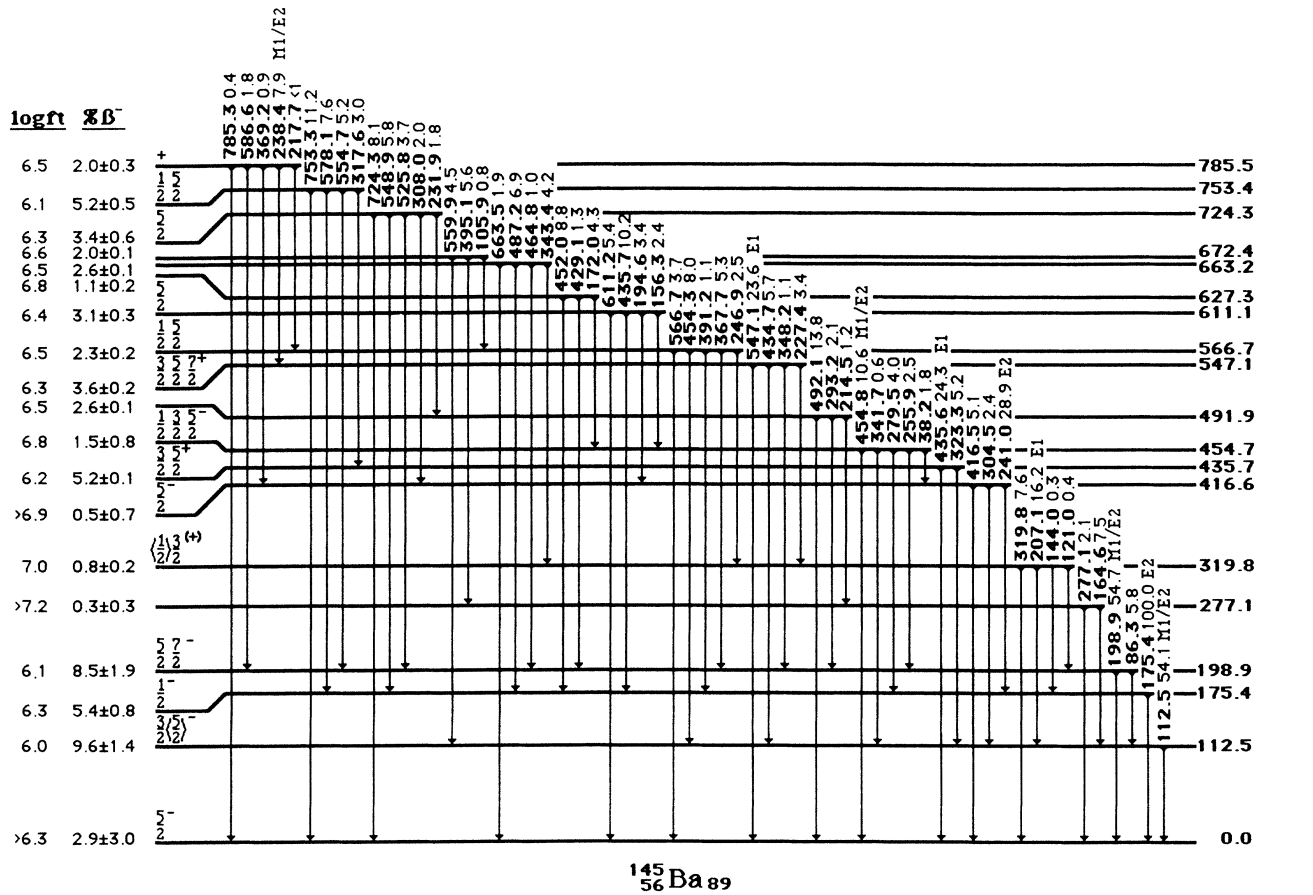

FIG. 4. Part 1 of the level scheme proposed for ^{145}Ba. Spin assignments are given for several of the low-lying levels. The beta intensities reported are from the gamma-ray transition intensity balances.

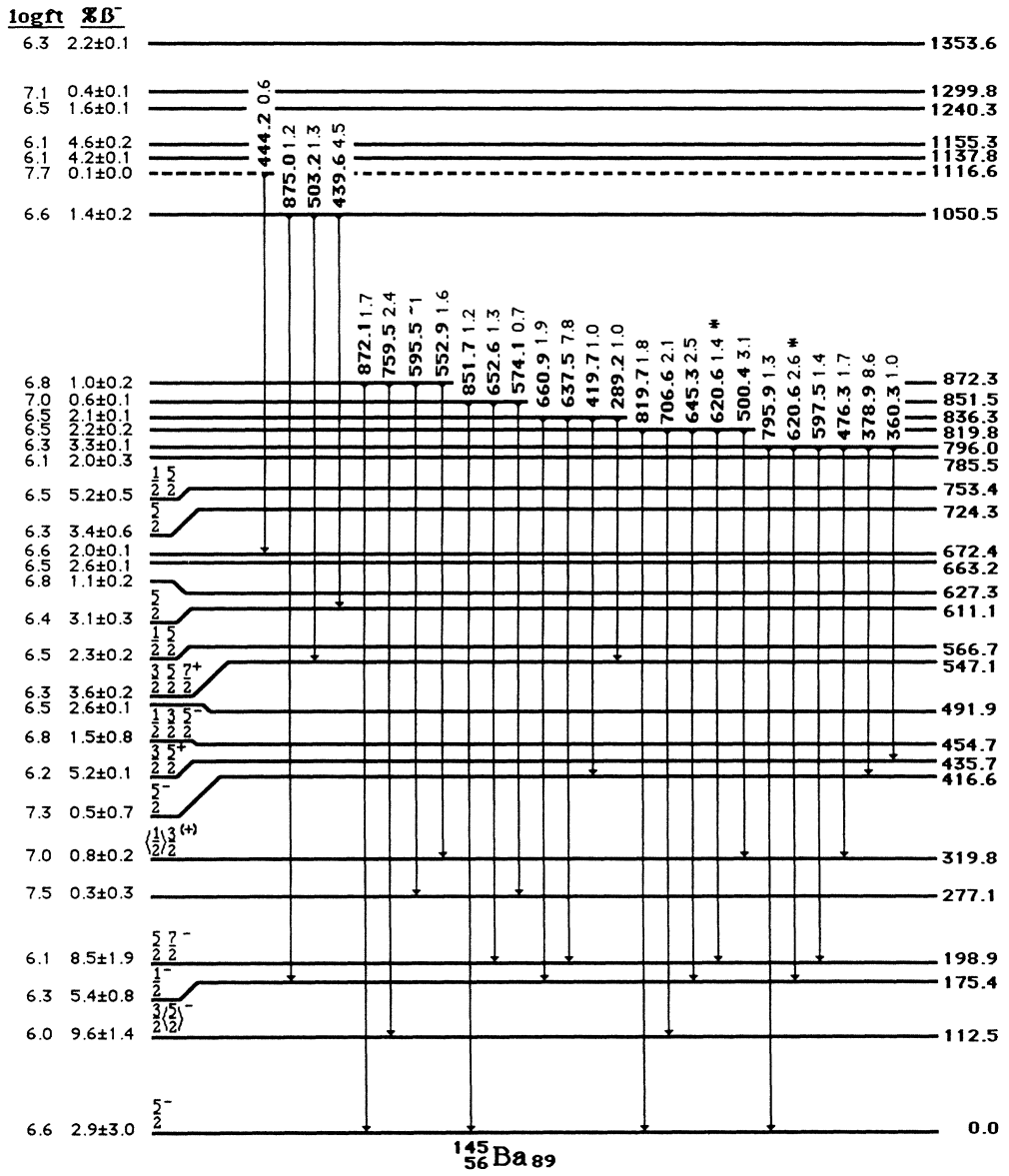

FIG. 5. Part 2 of the level scheme proposed for ^{145}Ba.

supported by the placement of at least three coincidences. Five new levels are proposed: the 627-, 1050-, 1116-, 1240-, and 1299-keV levels.[16] Because the 1116-keV level is supported by only one gamma transition, its placement is only tentative.

The 435-, 454-, and 620-keV γ rays are each placed twice in the ^{145}Ba level scheme. As can be seen from Fig. 2, the 435-keV gamma is clearly in coincidence with the 175-keV γ ray. The area of the 435-keV peak in the 175-keV gate, however, only accounts for 26% of the intensity of the 435-keV gamma. Because all of the transitions that feed the 435-keV level are also observed in the 435-keV coincidence gate, we conclude that there is also a 435-keV to ground transition. In the same manner, the 454-keV gamma is clearly seen in the 112-keV coincidence gate (Fig. 2). Again, however, the area of the 454-keV coincidence peak only accounts for 43% of the intensity of the 454-keV γ ray. The coincidence data indicate that there is a second 454-keV transition from the 454-keV level to the ground state. Finally, the 620-keV γ ray is seen in both the 175- and 199-keV coincidence gates and the area of the 620-keV peak in the two gates accounts for the total intensity observed in the singles spectra. The multiple placement of these three gamma rays is consistent with the previous work of Dejbakhsh.[16]

F. Spin and parity assignments

1. The ground state

The g.s. spin of ^{145}Ba, as mentioned earlier, has been measured to be $\frac{5}{2}$. The negative parity assignment for the g.s. is based upon the systematics of the $N=89$ isotones

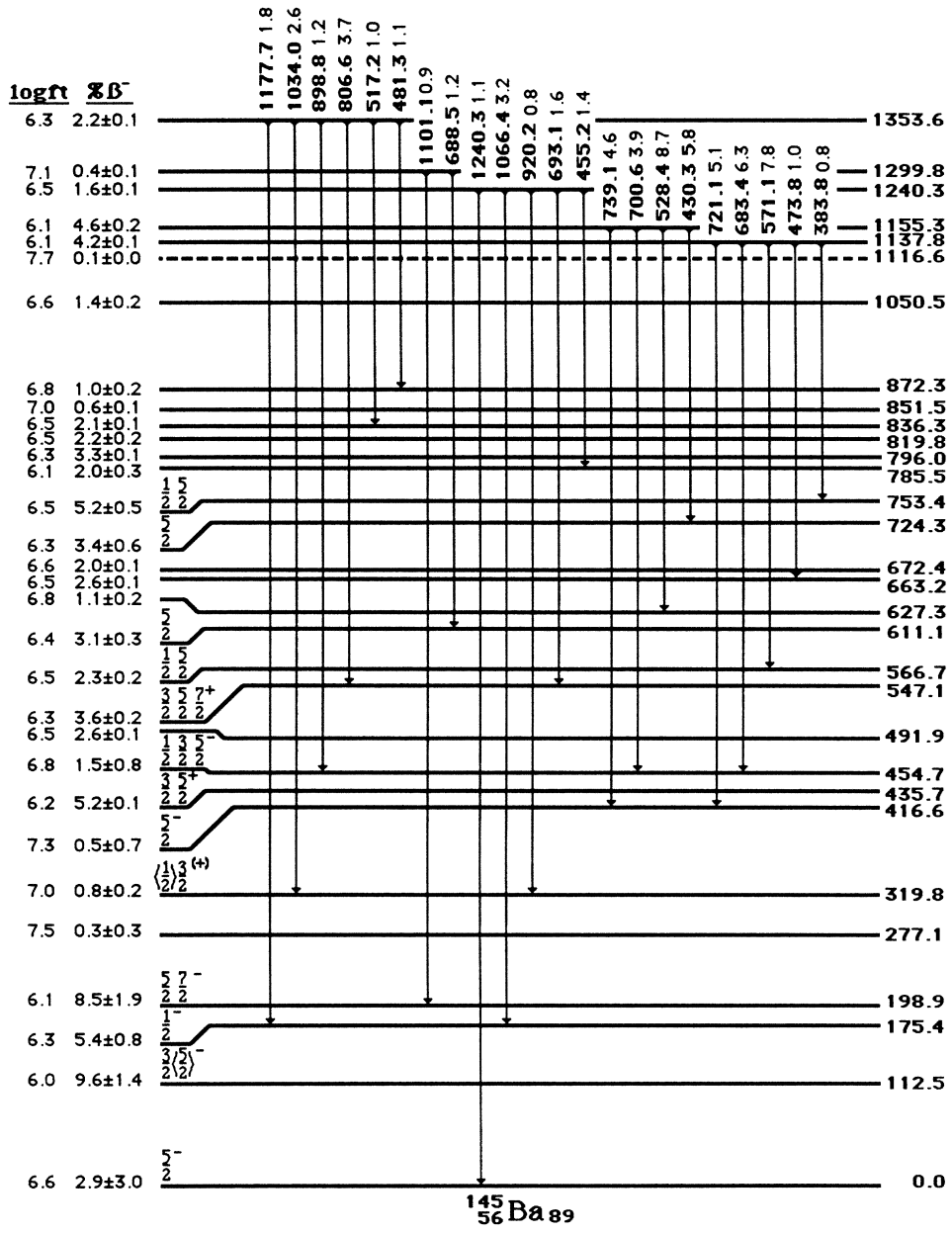

FIG. 6. Part 3 of the level scheme proposed for ^{145}Ba.

and the $Z=56$ isotopes. Both ^{149}Nd (Ref. 25) and ^{151}Sm (Ref. 26) have a g.s. J^{π} of $\frac{5}{2}^{-}$. The g.s. J^{π} of the odd-A Ba isotopes is ^{139}Ba$=\frac{7}{2}^{-}$,[27] ^{141}Ba$=\frac{3}{2}^{-}$,[28] and ^{143}Ba$=\frac{5}{2}^{-}$.[9] The deduced $\log f_0 t$ value of 6.6 for the g.s. is consistent with a first forbidden transition from the $\frac{3}{2}^{+}$ parent.[29]

2. The 112-keV level

The zero A_{44} values found in the four 112-keV gates (Table III) suggest that the spin of the 112-keV level is $\frac{3}{2}$; $A_{44}=0$ for any cascade with an intermediate spin of $\frac{3}{2}$. In addition, the $M1/E2$ multipolarity for the 112-keV transition implies that the parity of the 112-keV level is the same as that of the ground state. Finally, a $\log f_0 t$ of 6.0 is consistent with a first forbidden beta transition to the 112-keV level and the $\frac{3}{2}^{-}$ assignment.

3. The 175-keV level

The systematics of the first $\frac{1}{2}^{-}$ state in the Ba isotopes and in the $N=87$ isotones suggest that there should be a low-lying $\frac{1}{2}$ state in ^{145}Ba. The $\frac{1}{2}^{-}$ state drops from 1082 keV at one particle beyond the $N=82$ shell in ^{139}Ba to 34 keV in ^{143}Ba. Likewise, the first $\frac{1}{2}^{-}$ state drops from 576 keV to 34 keV across the $N=87$ isotones from ^{151}Gd to

^{143}Ba. The absence of any correlations in all six of the 175-keV angular correlation gates indicates that the 175-keV level is the spin $\frac{1}{2}$ level. There is no correlation when the intermediate level of a cascade has a spin of $\frac{1}{2}$. This assignment is consistent with the $E2$ multipolarity reported for the 175-keV transition.[30]

4. The 199-keV level

The spin and parity of the 199-keV level is limited to $\frac{3}{2}^-$, $\frac{5}{2}^-$, or $\frac{7}{2}^-$ by the multipolarity of the 199-keV transition. A spin assignment of $\frac{3}{2}^-$ is ruled out by the large, nonzero A_{44} values found for the 368-199, 554-199, and 637-199 cascades. The large A_{22} value observed for the 86-112 cascade suggests that the 199-keV level cannot have a $\frac{7}{2}^-$ spin; $A_{22} \leq 0.06$ for a $\frac{7}{2}(E2)\frac{3}{2}(M1/E2)\frac{5}{2}$ cascade. On the other hand, the large negative A_{22} value and positive A_{44} value found for the 637-199 cascade indicates that the 199-keV level has a spin of $\frac{7}{2}^-$ rather than $\frac{5}{2}^-$. This conflict is probably due to the drop in detection efficiency for the 86-keV transition, but our data cannot rule out the possibility that the 199-keV level has a spin of $\frac{5}{2}^-$. Because the A_{22}/A_{44} values from the remaining three 199-keV angular correlation gates are consistent with either assignment, we conclude that the 199-keV level has a spin of either $\frac{5}{2}^-$ or $\frac{7}{2}^-$.

5. The 319-keV level

The $E1$ multipolarity for the 207-keV transition limits the spin and parity of the 319-keV level to $\frac{1}{2}^+$, $\frac{3}{2}^+$, or $\frac{5}{2}^+$. The large, negative A_{22} value measured for the 207-112 cascade rules out a spin assignment of $\frac{5}{2}^+$; $A_{22} \geq -0.04$ for a $\frac{5}{2}^+(E1)\frac{3}{2}^-(M1/E2)\frac{5}{2}^-$ cascade. A spin of $\frac{1}{2}^+$ is also unlikely because $|A_{22}|$ for the above cascade is only within two sigma of the maximum theoretical $|A_{22}|$ value for a $\frac{1}{2}^+(E1)\frac{3}{2}^-(M1/E2)\frac{5}{2}^-$ cascade.

6. The 416-keV level

The nonzero A_{44} values found for the four 241-keV cascades indicate that the 416-keV level cannot have a spin of $\frac{3}{2}$. Likewise, the fact that any correlations were observed in the 241-keV gates negates a spin $\frac{1}{2}$ assignment for the 416-keV level. Consequently, because the 416-keV level feeds the $\frac{1}{2}^-$ 175-keV level, it must have a spin of $\frac{5}{2}$ and the 241-keV transition must therefore be an $E2$ transition. The measured 241-keV K conversion coefficient is consistent with either $M1$ or $E2$ multipolarity and the $\frac{5}{2}^-$ assignment. The 241- α_L/α_K ratio of 0.09 ± 0.02, is closer to the theoretical value for an $M1$ (0.14) rather than an $E2$ (0.23) transition. This discrepancy is probably a result of the large uncertainty (14% and 12%, respectively) in α_K and α_L for the 241-keV transition.

7. The 435-keV level

The spin and parity of the 435-keV level is limited to $\frac{3}{2}^+$, $\frac{5}{2}^+$, or $\frac{7}{2}^+$ by the $E1$ multipolarity of the 435-keV gamma. A $\frac{7}{2}^+$ assignment is unlikely because of the large beta feeding to the 435-keV level. For the spin to be $\frac{7}{2}^+$, the measured $\log f_0 t$ would have to be approximately 11 rather than 6. If the 260-keV transition observed in the 175-keV coincidence gate does feed out of the 435-keV level, then the 435-keV level must have a spin of $\frac{3}{2}^+$; an $M2$ transition of this magnitude (0.9) would have been observed in the c.e. spectrum. However, because the 260-keV line is not observed in the 317-keV coincidence gate, we could not conclude that there is a transition from the 435- to the 175-keV level. Our calculations indicate that the 260-keV peak should have been easily seen in the 327-keV gate if it does feed out of the 435-keV level. In addition, the A_{22} value found for the 317-435 cascade is within one σ of the value expected for a $\frac{5}{2}^+$ spin and only within two σ's of the value for a spin of $\frac{3}{2}^+$. For this reason, and because of the uncertainty in the placement of the 260-keV gamma, we conclude that the 435-keV level may have a spin of either $\frac{3}{2}^+$ or $\frac{5}{2}^+$.

8. The 454- and 547-keV levels

The measured multipolarity of both the 454- and 547-keV transitions limits the spins of the 454- and 547-keV levels again to either $\frac{3}{2}$, $\frac{5}{2}$, or $\frac{7}{2}$. The $M1/E2$ character of the 454-keV transition implies that the 454-keV level has the same parity as the ground state. The $E1$ multipolarity of the 547-keV transition indicates that the 547-keV level has the opposite parity of the ground state.

9. The 566- and 753-keV levels

The spins of both the 566- and 753-keV levels can be limited to either $\frac{1}{2}$ or $\frac{5}{2}$ once the 199-keV level is known to have a spin of $\frac{5}{2}$ or $\frac{7}{2}$. A spin of $\frac{7}{2}$ can be ruled out because A_{44} is always greater than or equal to zero for either a $\frac{7}{2}$-$\frac{5}{2}$-$\frac{5}{2}$ or $\frac{7}{2}$-$\frac{7}{2}$-$\frac{5}{2}$ cascade; A_{44} is clearly greater than zero for both the 367-199 and 554-199 cascades. Likewise, a $\frac{3}{2}$ assignment can be ruled out for both levels because A_{44} is also always less than or equal to zero for a $\frac{3}{2}$-$\frac{5}{2}$-$\frac{5}{2}$ and a $\frac{3}{2}(E2)\frac{7}{2}$-$\frac{5}{2}$ cascade.

10. The 611- and 724-keV levels

Finally, the 611- and 724-keV levels have a spin of either $\frac{1}{2}$, $\frac{3}{2}$, or $\frac{5}{2}$ as both of these levels feed the $\frac{1}{2}$ 175-keV level. The negative A_{22} values observed for both the 194-241 and 308-241 cascade rule out the possibility that either level has a spin of $\frac{1}{2}$; $A_{22} \geq 0$ for a $\frac{1}{2}$-$\frac{5}{2}$-$\frac{1}{2}$ cascade. Likewise, the positive A_{44} values for the above cascades negates a spin $\frac{3}{2}$ assignment for either level as $A_{44} \leq 0$ for a $\frac{3}{2}$-$\frac{5}{2}$-$\frac{1}{2}$ cascade. Consequently, the 611- and 724-keV levels must both have a spin of $\frac{5}{2}$.

IV. CONCLUSION

The systematics of the low-lying levels in the $N=89$ isotones are shown in Figs. 7 and 8. The octupole rotational structure marked by parity doublets in the light odd-A actinides is not readily identified in ^{145}Ba. Like ^{149}Nd (Ref. 25) and ^{151}Sm (Ref. 26), the low-lying levels in

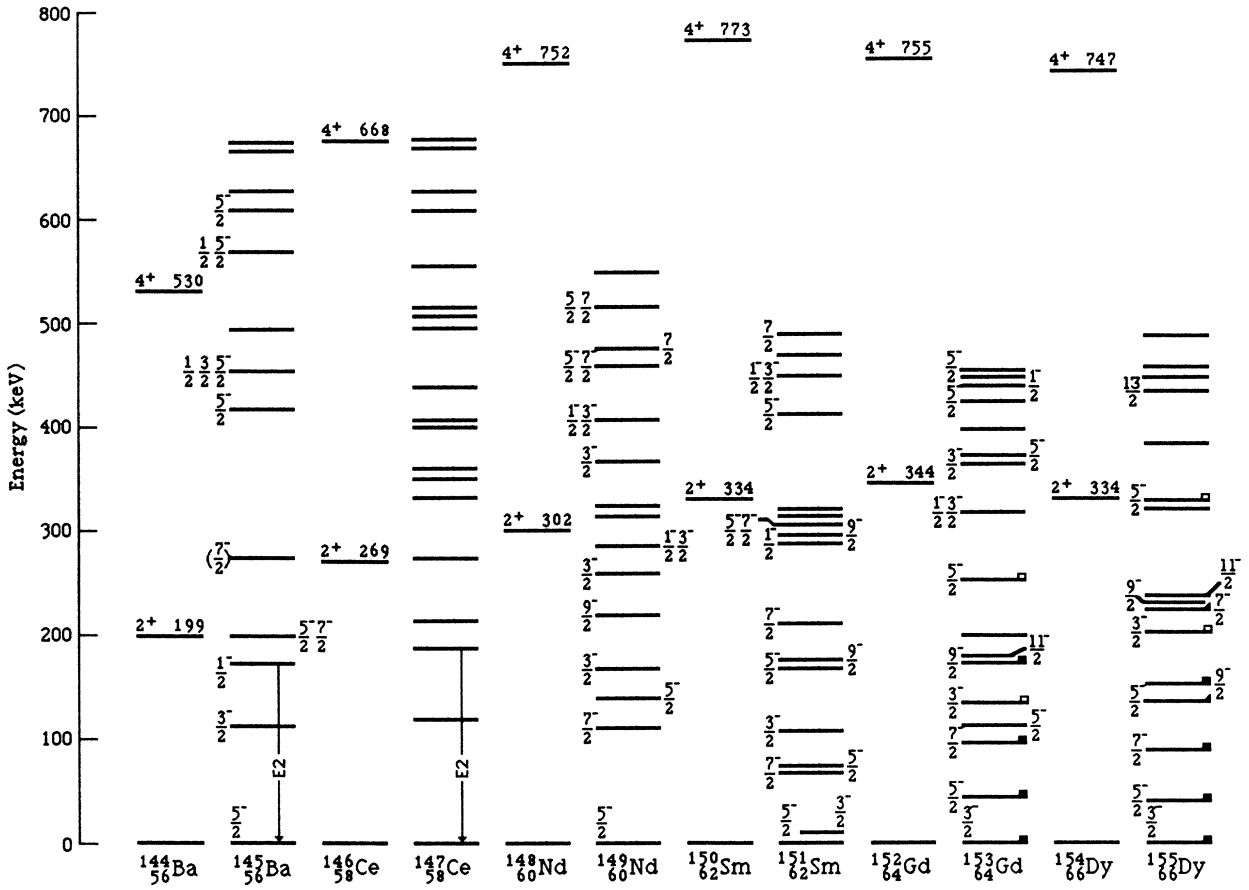

FIG. 7. Systematics of the negative parity states in the $N=89$ isotones. The rotational bands in ^{153}Gd and ^{155}Dy are identified by the characters attached to the levels.

^{145}Ba cannot be grouped into any obvious rotational bands consistent with the structure of the higher Z nuclides. Rotational structure is not observed in the $N=89$ isotones until ^{153}Gd and ^{155}Dy.[31,32]

One explanation of the structure observed in ^{145}Ba is that the low-lying energy levels simply arise from collective vibrations. As can be seen in Fig. 7, the energies of the first group of negative parity levels are clustered around the 199-keV energy of the first 2^+ level in the ^{144}Ba core. Moreover, the energies of the second group of negative parity states are clustered around the 580-keV 4^+ level in the core. The positive parity states, in contrast, clearly lie below the 759-keV 1^- level in ^{144}Ba (Fig. 8). These levels, however, could be pushed down in energy by some type of intermediate particle-core interaction involving the $h_{11/2}$ proton and $h_{9/2}$ neutron spin orbit partner orbitals. A second, and perhaps more serious problem, with a vibrational interpretation of the low-lying structure, is the $\frac{5}{2}^-$ ground state. If ^{145}Ba is a spherical vibrator, then one would expect the g.s. to be $\frac{7}{2}^-$ or $\frac{9}{2}^-$. The g.s. of $\frac{5}{2}^-$ could arise from a three-hole $f_{7/2}$ cluster similar to the $(f_{7/2})^3$ cluster states found in the $N=85$ isotones.[33] The $\frac{5}{2}^-$ state of the cluster, is then pushed below the $\frac{7}{2}^-$ or $\frac{9}{2}^-$ state in the same way that the $\frac{3}{2}^-$ state is pushed below the $\frac{7}{2}^-$ state in the $N=85$ isotones. A relatively strong interaction, however, would be required to account for the $\frac{1}{2}^-$ 175-keV level with an $(f_{7/2})^3$ cluster ground state.

A second interpretation of the low-energy structure in ^{145}Ba is to group the levels at 112, 175, 277, and 416 keV into a decoupled $K=\frac{1}{2}^-$ band. The energies of the levels in the band are described by the equation

$$E(J)=A^*J(J+1)+a^*A^*(-1)^{J+1/2}(J+\tfrac{1}{2})+C\ ,$$

with the rotational parameter $A=20.3$ keV, the decoupling parameter $a=-2.0$, and $C=118.5$ keV. It should be noted that, although no spin was assigned to the 277-keV level, it is a good candidate for the $\frac{7}{2}^-$ member of the $K=\frac{1}{2}^-$ band. The decay of the 277-keV level is consistent with a $\frac{7}{2}^-$ assignment in that it only feeds the $\frac{3}{2}^-$ 112-keV level and the $\frac{5}{2}^-$ g.s.; it does not feed the $\frac{1}{2}^-$ 175-keV level. In addition, the small beta feeding and $\log f_1 t$ of 9.6 for the 277-keV level are consistent with a first forbidden transition from the $\frac{3}{2}^-$ parent and a spin of $\frac{7}{2}^-$.

The rotational parameter of 20 keV for the $K=\frac{1}{2}^-$ band is the right magnitude for this region as A ranges from 7 to 20 keV for the rotational bands in ^{153}Gd and ^{155}Dy. Likewise, the decoupling parameter of -2.0 matches the values predicted from simple Nilsson calculations for the $[530]\frac{1}{2}$ orbital.[34] The most obvious candi-

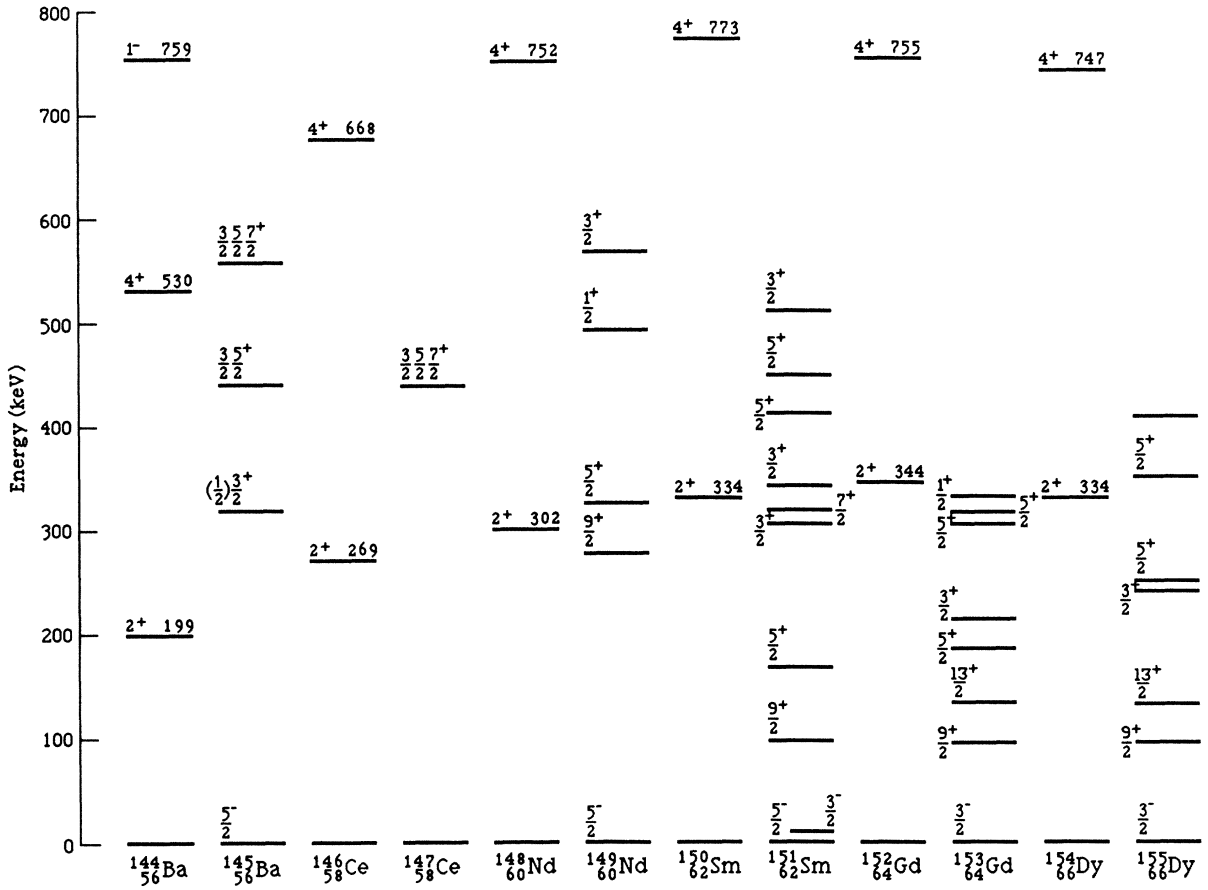

FIG. 8. Systematics of the positive parity states in the $N=89$ isotones.

date for a $K=\frac{1}{2}^-$ band seven particles beyond the $N=82$ shell is the $[530]\frac{1}{2}$ orbital as it lies very near the Fermi surface. The level at 199 keV might be the first member of a band built upon the $\frac{5}{2}^-$ g.s., if the 199-keV level has a spin of $\frac{7}{2}^-$. The rotational parameter for this band would be about 28 keV.

There are two serious problems with this interpretation of the low-lying structure observed in ^{145}Ba. First of all, the rotational parameters for the two proposed negative parity bands are rather large and indicate that ^{145}Ba is only weakly quadrupole deformed. This conclusion is also supported by the fact that the β_2 values calculated from the lifetimes of the first 2^+ states in ^{144}Ba and ^{146}Ba are consistent with small deformation. The β_2/β_{2sp} ratio for ^{144}Ba and ^{146}Ba is 6.8 and 7.5, respectively, compared to the ratio of 12.2 and 10.7 found in the quadrupole deformed nuclei ^{154}Gd and ^{156}Dy.[35] In contrast, the decoupling parameter found for the $K=\frac{1}{2}^-$ band indicates that ^{145}Ba is well deformed with $\beta_2\simeq 0.3$. This discrepancy is even worse when octupole deformations are included in the Nilsson calculations of the decoupling parameter, as Leander *et al.* predict that a decoupled band built on the $[530]\frac{1}{2}$ Nilsson orbital should have $a=1.4$ if the nucleus is octupole deformed.[9] Secondly, the low-lying positive parity levels are difficult to explain from a rotational viewpoint. If the $K=\frac{1}{2}^-$ band is a decoupled band similar to those observed in the octupole deformed light actinides, then one would expect to observe a $K=\frac{1}{2}^+$ band in ^{145}Ba near the $K=\frac{1}{2}^-$ band. No decoupled band, however, can be built upon any of the positive parity levels with a decoupling parameter of approximately 2 and a rotational parameter of 10–20 keV.

Like ^{147}Ce and ^{149}Nd, the low-lying structure in ^{145}Ba cannot be readily described in the framework of the standard Nilsson model which includes only quadrupole deformation. Because these $N=89$ transitional nuclei are only weak, quadrupole deformed, higher orders of deformation may play a large role in determining their structure. Thus, although no parity doublets are observed as predicted, it is possible that one must still include octupole deformation in the Nilsson basis in order to reproduce the observed structure in this transitional region. Clearly, more theoretical work is needed to gain an understanding of this region.

ACKNOWLEDGMENTS

This work was supported in part by the U.S. Department of Energy under Contracts No. DE-AS05-79ER10494 and No. DE-AC02-76CH00016. We are grateful for the many helpful discussions with Dr. G. A. Leander during the preparation of this paper.

*Present address: Institute for Nuclear Studies, 05-400 Swierk, Poland.

†Present address: Cyclotron Institute, Texas A&M University, College Station, TX 77843.

[1]L. J. Rainwater, Phys. Rev. **79**, 432 (1950).

[2]G. A. Leander, R. K. Sheline, P. Möller, P. Olanders, I. Ragnarsson, and A. J. Sierk, Nucl. Phys. A**388**, 452 (1983).

[3]F. Iachello and A. D. Jackson, Phys. Lett. **108B**, 151 (1982).

[4]M. Gai, J. F. Ennis, M. Ruscev, E. C. Schloemer, B. Shivakumar, S. M. Sterbenz, N. Tsoupas, and D. A. Bromley, Phys. Rev. Lett. **51**, 646 (1983).

[5]W. Nazarewicz, P. Olanders, I. Ragnarsson, J. Dudek, G. A. Leander, P. Möller, and E. Ruchowska, Nucl. Phys **A429**, 269 (1984).

[6]G. A. Leander and R. K. Sheline, Nucl. Phys. **A413**, 375 (1984).

[7]R. R. Chasman, Phys. Rev. **96B**, 7 (1980).

[8]I. Ahmad, J. E. Gindler, R. R. Betts, R. R. Chasman, and A. M. Friedman, Phys. Rev. Lett. **49**, 1758 (1982).

[9]G. A. Leander, W. Nazarewicz, P. Olanders, I. Ragnarsson, and J. Dudek, Phys. Lett. **152B**, 284 (1985).

[10]F. Stephens, F. Asaro, and I. Perlman, Phys. Rev. **96**, 1568 (1954).

[11]A. C. Mueller, F. Buchinger, W. Klempt, E. W. Otten, R. Neugart, C. Ekström, and J. Heinemeier, Nucl. Phys. **A403**, 234 (1983).

[12]I. Ragnarsson, Phys. Lett. **130B**, 353 (1983).

[13]R. K. Sheline, D. Decman, K. Nybø, T. F. Thorsteinsen, G. Lovhøiden, E. R. Flynn, J. A. Cizewski, D. K. Burke, G. Sletten, P. Hill, N. Kaffrell, W. Kurcewicz, G. Nyman, and G. A. Leander, Phys. Lett. **133B**, 13 (1983).

[14]R. K. Sheline and G. A. Leander, Phys. Rev. Lett. **51**, 359 (1983).

[15]M. S. Rapaport, G. Engler, A. Gayer, and I. Yoresh, Z. Phys. A **305**, 359 (1982).

[16]H. Dejbakhsh, Ph.D. thesis, University of Oklahoma, 1985.

[17]R. L. Gill and A. Piotrowski, Nucl. Instrum. Methods A **234**, 213 (1985).

[18]A. Piotrowski, R. L. Gill, and D. C. McDonald, Nucl. Instrum. Methods **224**, 1 (1984).

[19]J. K. Tuli, Nucl. Data Sheets **29**, 533 (1980).

[20]P. L. Reeder, Brookhaven National Laboratory Report No. BNL-51778, p. 358, 1983 (unpublished).

[21]B. Pfeiffer, F. Schussler, J. Blachot, S. J. Feenstra, J. van Klinken, H. Lawin, E. Monnand, G. Sadler, H. Wollnik, and K. D. Wünsch, Z. Phys. A **287**, 191 (1978).

[22]D. C. Camp and A. L. VanLehn, Nucl. Instrum. Methods **76**, 192 (1969).

[23]N. B. Gove and M. J. Martin, Nucl. Data Tables **10**, 205 (1971).

[24]B. Pahlmann, U. Keyser, and F. Münnich, Z. Phys. A **308**, 345 (1982).

[25]J. A. Pinston, R. Roussille, G. Sadler, W. Tenten, J. P. Bocquet, B. Pfeiffer, and D. D. Warner, Z. Phys. A **282**, 303 (1977).

[26]W. B. Cook, M. W. Johns, G. Lovhøiden, and J. C. Waddington, Nucl. Phys. A**259**, 461 (1976).

[27]L. K. Peker, Nucl. Data Sheets **32**, 42 (1981).

[28]L. K. Peker, Nucl. Data Sheets **45**, 69 (1985).

[29]C. Thibault, F. Touchard, S. Büttgenbach, R. Klapisch, M. De Saint Simon, H. T. Duong, P. Jacquinot, P. Juncar, S. Liberman, P. Pillet, J. Pinard, J. L. Vialle, A. Pesnelle, and G. Huber, Nucl. Phys. A**367**, 1 (1981).

[30]F. Schussler, B. Pfeiffer, H. Lawin, E. Monnand, J. Munzel, J. A. Pinston, K. Sistemisch, in *Proceedings of the Fourth International Conference on Nuclei Far from Stability*, edited by P. G. Hansen and O. B. Nielsen (Skolen, Helsingør, 1981), p. 589.

[31]M. A. Lee, Nucl. Data Sheets **37**, 487 (1982).

[32]L. A. Kroger and C. W. Reich, Nucl. Data Sheets **15**, 409 (1975).

[33]J. D. Robertson, W. B. Walters, S. F. Faller, C. A. Stone, R. L. Gill, and A. Piotrowski, Z. Phys. A **321**, 705 (1985).

[34]J. M. Irvine, *Nuclear Structure Theory* (Pergamon, New York, 1972), p. 333.

[35]*Table of Isotopes*, 7th ed., edited by C. M. Lederer and V. S. Shirley (Wiley, New York, 1978).

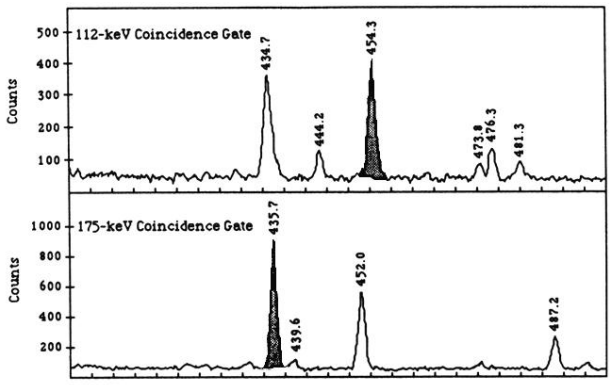

FIG. 2. Portions of the 112- and 175-keV γ-γ coincidence gates.